Annals of Academy of Romanian Scientists
Series: Medical Sciences
ISSN 2067-7766 *Volume 2, Number 2/2011*

Original Article

EVALUATION OF MICROMOUVEMENT IN THE BIOMECHANICAL CONTEXT OF BONE SHAFT FRACTURE HEALING IN ELASTIC VERSUS RIGID FIXATIONS

Radu Dan NECULA[*)1], Gheorghe PANAIT[2], Ioan SZÁVA[3], Iosif ŞAMOTĂ[4]

1) „Transilvania" University of Brasov, Medicine Faculty, Orthopaedic and Traumatology Dept.
2) „Carol Davila" University of Medicine Bucharest, Orthopaedic and Traumatology Dept.
3) „Transilvania" University of Brasov, Strength of Materials and Vibration Dept.

Abstract

Fixation of long bone fractures, especially in the middle part, requires respect to some biomechanical conditions. Flexible fixation from the biological point of view it seems to be the method of choice. So as an experimental support of our good clinical results we started on Video Image Correlation investigation of mechanical condition, to determine the corresponding individual displacements and strains of different method of fixation. The obtained results offered several important and useful biomechanical conclusions.

Keywords: *strain, rigid fixation, flexible fixation*

Rezumat

Fixarea internă a fracturilor diafizare ale oaselor lungi necesită respectarea unor condiții biomecanice specifice. Din punctul de vedere al mediului biologic particular porțiunii medii diafizare, fixarea elastică pare să fie metoda de elecție. Pentru confirmarea rezultatelor bune clinice ale fixării elastice centromedulare, am investigat printr-o metodă modernă experimentală (Video Image Correlation) deplasările specifice ce apar în focarul de fractură fixat cu implanturi în condiții diferite de rigiditate. Rezultatele experimentale oferă posibilitatea unor concluzii practice importante privind comportamentul biomecanic al diferitelor mijloace de fixare ale fracturilor.

Cuvinte-cheie: *deformare specifică, fixare rigidă, fixare elastică*

[*)] ***Author for correspondence:*** *Necula Radu Dan, e-mail: ortomed.bv@gmail.com*

Introduction

The healing of the shaft bone fracture are determining by the energy of the fracture, the biomechanical milieu created by the fixation device, the accuracy of selected fixation technique, the general and local disease interacting with fracture healing process, and not the last the patient compliance. The energy of impact induce the fracture configuration and biological condition around the fracture site; in high energy fractures one of most biological purpose is to protect the residual blood supply of the affected bone.

Different methods of internal fixation were compared in biomechanical studies: analyses of external fracture fixation devices rigidity on fracture healing (1, 4, 13), compression plates fixation (5, 6, 8, 12), locking plates fixation (3), intramedullary nails or comparison between different kind of fixation (7, 11). The biomechanical environment created by the fixation device is depending upon the quality of fracture reduction and stability in rigid fixations; the stiffness of fracture device and consequent promotes stress and strain at the fractured bone ends under functional loading in flexible fixation. It is known that mechanical environmental changes modulate the biomechanical fracture healing (2).

Method

The VIC method is based on analyzing of two, simultaneously captured images by means of two video cameras. Similarly, with the human eyes, we will obtain a spatial (3-D) image of the analyzed specimen. In principle, the VIC-3D consists of two, high-resolution video cameras (disposed symmetrically in comparison to the analyzed specimen), on a high-rigidity aluminum rod, mounted on a very stable tripod.

The specimen, covered in advance with a special paint, spread irregularly in small drops, will offer an easy recognition of these small drops and consequently: of the displacement of the corresponding points of the specimen. After the calibration of the video cameras in the specimen's viewing plane, the software will be able recognizing and identifying, with 1 *micron* accuracy, the observed points spatial displacements from the specimen's surface.

The substitution of the calibration plate with the tested specimen allows capturing, with these two cameras, of individual and simultaneously images of the specimen. Each camera offers images constituted from matrixes of $[n \cdot m]$ pixels. Adopting a pre-selection of the reference cell (here: $5 \cdot 5$ pixels) and an adequate step of its moving, the whole captured image will be scanned. The software offers for each (step-by-step) position of the reference cell an unique grey-code, corresponding to the central pixel of the cell. This unique grey-code allows an easy identification of the motion (displacement) of this cell during the specimen's loading process.

After the loading cycle, in order to analyze the completely 3D displacement field of the tested specimen, it will be necessary the identification of a single point (which is usually pre-marked on the specimen's surface by a small cross) from the two cameras captured images (figure no.1). The accuracy of the displacements' evaluation depends on the pre-selected cell's size and its scanning step. The obtained information (displacements, strains etc), presented like color maps (similarly with the FEM analysis results), graphs, respectively can be exported in Excel-files for further analysis. The VIC-3D allows full-field evaluation of the displacements, between several microns and centimeters.

Analyzed samples have followed an osteotomies protocol summarized in Table 1. All osteotomies were applied to the third medium shaft being used in both preserved human bones (tibia and femurs preserved, provided for experimental purposes in Preclinical Department of Braşov Faculty of Medicine) and fresh bovine bones (femurs).

Table 1: Osteotomies and fixations protocol

Exp. code	Bone	Osteotomy	AO type	Fixation device
F_1	femur	Simple oblique	32A2	Dynamic compression plate (+ bending)
T_1	tibia	Simple oblique	42A2	Dynamic compression plate (- bending)
F_{1c}	femur	Wedge osteotomy	32B2	Neutralization plate
T_{1c}	tibia	Wedge fracture	42B2	Neutralization plate
F_{1b}	femur	Complex irregular osteotomy	32C3	Bridge plate
F_{2Fe1}	femur	Wedge osteotomy	32B2	External fixator
T_K	tibia	Simple oblique	42A2	Reamed nail
T_{Kc}	tibia	Wedge osteotomy	42B2	Reamed nail
F_2	tibia	Simple oblique	42A2	Flexible nails
F_{2c}	tibia	Wedge osteotomy	42B2	Flexible nails
F_{2T}	femur	Wedge osteotomy	32B2	Unreamed static locked nail
V_2	bovine femur	Simple oblique	A2	Dynamic compression plate (Ti)
V_3	bovine femur	Simple oblique	A2	LCP plate as internal fixator (Cr)
V_1	bovine femur	Simple oblique	A2	LCP plate as internal fixator (Ti)

The authors marked significant points at the both sizes of the fracture. The fractured bones, subjected to compression up to 400 *N* in a universal tensile-compression testing machine, were monitored during several cycles of loading and unloading (figure no. 1, 2). Based on the initial data of the specimens (unloaded stage), the authors determined the corresponding individual and relative displacements and strains of these significant points, respectively the fixing solution biomechanical behavior (and its efficiency) from the micro-movements point of view in the fractured zone. The obtained results offered several important and useful biomechanical conclusions, applicable by the medical members of the authors' team (figure no 3).

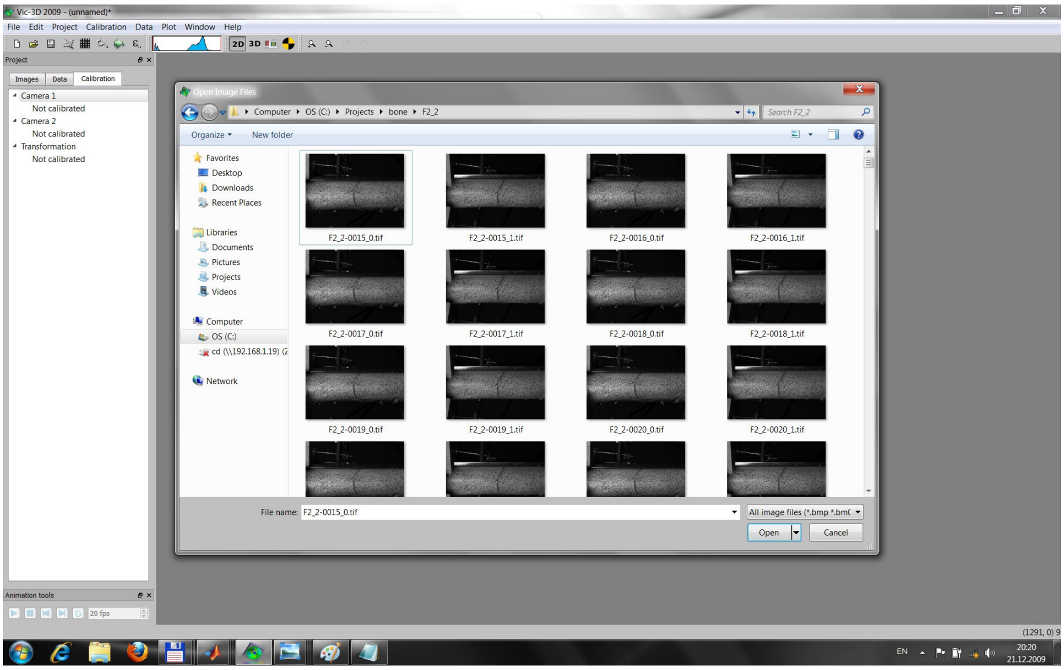

Figure 1: Video images of the tested specimen, obtained with the VIC-3D system, corresponding to F2_2-0015_0.tif ... F2_2 -0352_1.tif

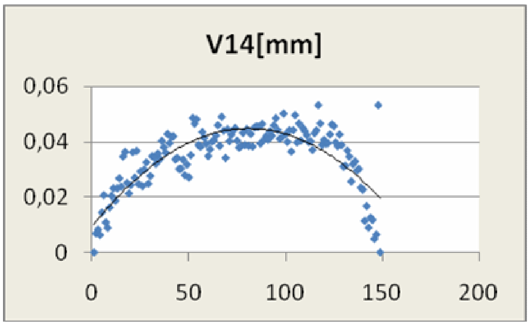

Figure 1: The evolution of movements over the 150 records between 0-420-0 N for point 14 on the radial axis (v). Extract the corresponding average value of the loading point 63 (400N)

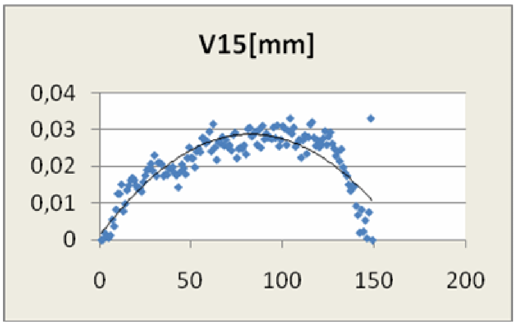

Figure 2: The evolution of movements over the 150 records between 0-420-0 N for point 15 on the radial axis (v). Extract the corresponding average value of the loading point 63 (400N)

Based on a detailed analyze of the micro-movements shape, tendency and amplitude, the authors obtained several useful clinical information. The differences of the monitored values represent the relative displacement at the level of the fracture's zone (along *x*-, respectively *y-axis*), and based on them, became possible the corresponding strains evaluation. The strain is the most near expression of the micro-movements in the fracture zone. So, a (Δx_1) displacement between the extremities of a complex irregular fracture can present a strain below of a simple fracture strain with a gap (Δx_2) with $\Delta x_2 < \Delta x_1$.

The importance of strain was developed by Peren (9, 10), referring to fracture gap space. Thus, the specific deformation fracture gap space (strain) is the ratio of relative deformation and distance ΔL initial gap L. According to this theory a strain under 2% (limit value supported by cortical bone) leads to direct healing. Lamellar bone can tolerate up to 10% deformation and in this specific micro-movements area will occur indirect healing with voluminous periosteal callus formation. A displacement in the fracture gap that exceeds this value leads to nonunion. Such fixing methods, that limit the specific movements and ε_x and ε_y below 0.02 will lead to direct healing, those between 0.02 and 0.1 will create the conditions for indirect healing, and those that exceed 0.1 will require further analysis of biomechanical environment for reporting the causes that lead to nonunion.

Results

1. In case of *dynamic compression plate fixation* for the first the experiment simulate a type AO 42-A2 fracture fixed with DCP plate with 12 screws (11 screws were applied), with external compression and pre-bending (about 2*mm* plate pre-bending on the central part). The longitudinal strain (ε_x) is limited near the plate by the stiffness of the plate; with distance from the plate, will record higher values (Figure no 4). The movements in radial direction, transverse at first load, expressed a tendency to relative slip between parts, controlled by the plate (Figure no 5).

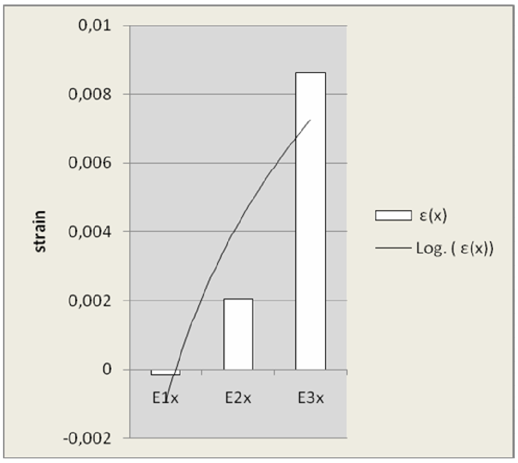

Figure 4: Longitudinal strain

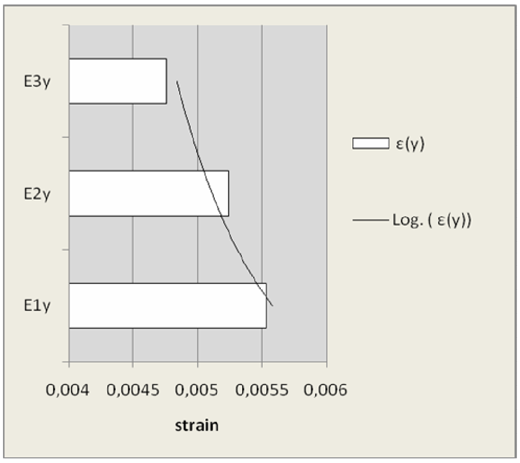

Figure 5: Radial strain

So, we have to start higher radial strain next to plate, with a desire by cancel out the lag screws; then, the phenomenon reverse, i.e. greater radial strain on the opposite side the plate; finally we found that the system enters to normal working condition with practically negligible effect (10% of maximum of higher strain), with remaining predominant compressive longitudinal micro-movements.

2. In case of *dynamic compression plate fixation without over-bending*, was simulated a 32-A2 fracture type AO DCP plate fixed with 10 screws. There were applied 8 screws due to our protocol not to apply the lag screw, with external compression, but without over-bending the plate. Fixation with plate without overbending, on the principle of fracture compression, and loading at 400*N* involves more extensive strain, than on the opposite side (figure no.6). It can observe that on the opposite side occurs stress relieve when compression is applying by plate fixation with values of strain (ε_x= 0.02192) compared with those observed in the model with overbending (ε_x= -0.008634). Basically, over-bending of the plate reduces to 40% the longitudinal strain.

The biomechanical behavior in terms of radial strain leads to conclusions that the maximum displacement amplitude is located at values of 16% when compared over-bending plate with plate fixation without over-bending. In terms of type of micro-movement occurred on the axis Y, is found that with over-bending of the plate displacement occurs as a sliding between the surfaces and in the absence of over-bending appears as a rotational movement, centered on the longitudinal axis of the plate and in this case exceeded the limit value of 0.02% of gap strain under stabile fixation (figure no.7).

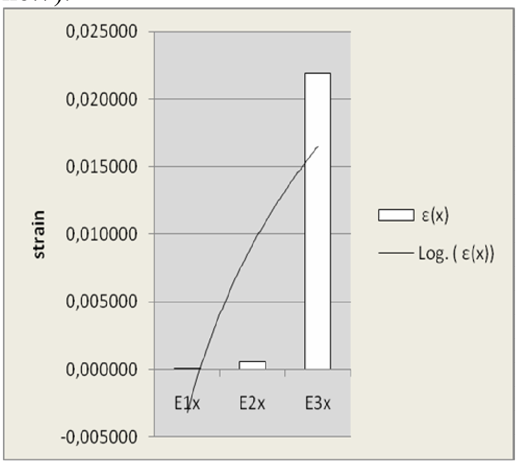

Figure 6: Longitudinal strain

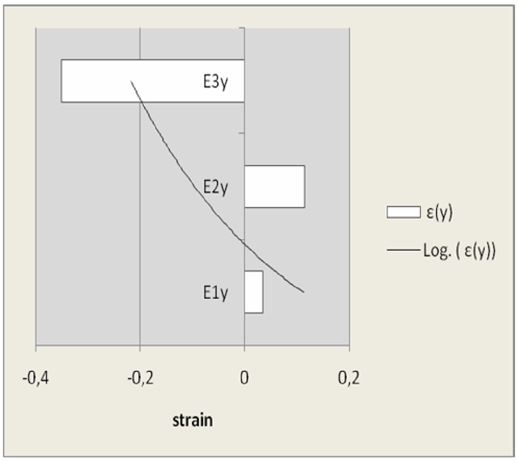

Figure 7: Radial strain

3. The *protection plates* were tested likewise. Experimental, a wedge fracture type AO B2, was simulated by two excluding oblique osteotomies. Two samples were prepared as a femur and tibia. Femur fixation consisted of a neutralization plate with 10 screws (intermediary fragment was not fixed to be able to evaluate the trend of strain and assess the protective role of the plate). Technical intermediate fragment was attached with silicone glue, which does not affect the results of its mechanical characteristics. Tibia was fixed by a neutralization plate (intermediate fragment stabilize by two lag screws placed through the plate). Six levels were selected to perform measurements, ε (X, Y) for strain between the main fragments, ie ε (X, Y) for strain of intermediate fragment against one of the main fragments.

If protection plate fixation is used, it was noted that on the opposite side the plate, longitudinal strain of intermediate fragment presented higher values than the main fragments [$\varepsilon_{(X)i} > \varepsilon_{(X)}$] and therefore wedge effect occurs (figure no. 8 and 9). The values of these movements are the expression of the protective role of the plate, which discharges most of the axial loading. In radial direction, the strain are insignificant for the main fragments, but intermediate fragment has a wedge effect, blocked by plate, with maximum of $\varepsilon_{(y)i}$ immediately below the plate (E_{1y} = 0.228359).

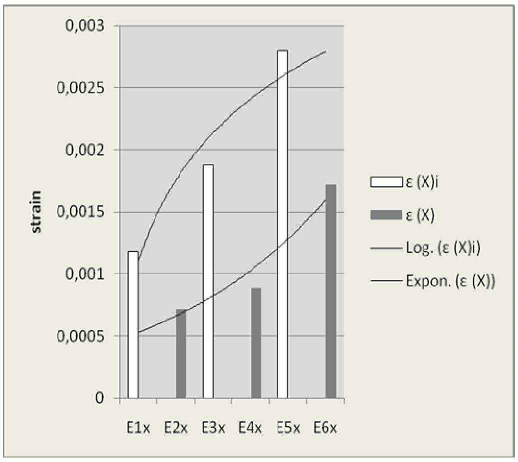

Figure 8: Longitudinal strain

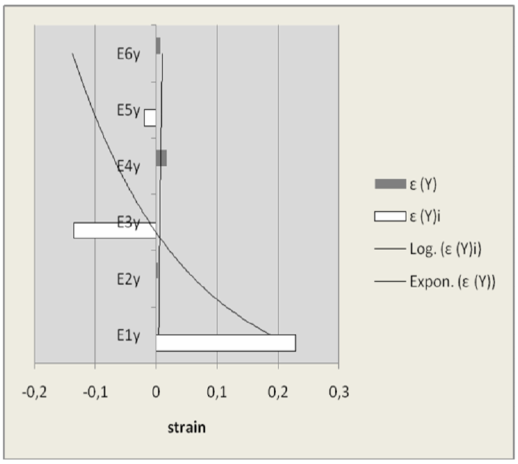

Figure 9: Radial strain

The same phenomenon as the femur can be seen in the case of tibia, but with higher magnitudes, due to reduced cross section compared with the femur (figure no. 10, 11). However, due to stabilization of intermediate fragment with lag screw, the wedge effect is greatly diminished, with values of fracture gap radial strain $\varepsilon_{(y)i}$ compatible with direct healing (E_{5y} = -0.01982).

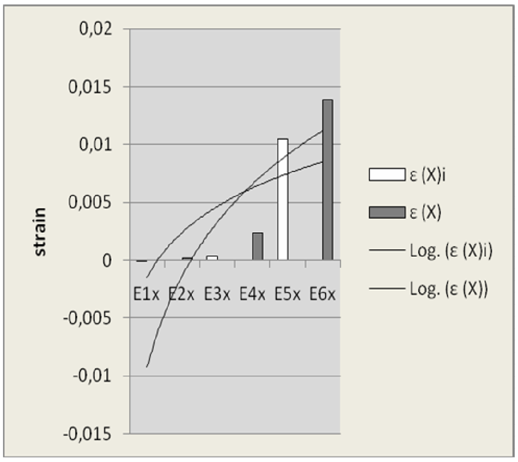

Figure 10: Longitudinal strain

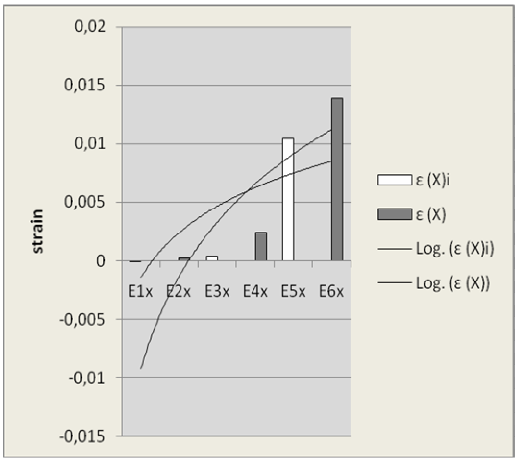

Figure 11: Radial strain

4. The biomechanics of *bridge plate fixation* impose high unstable osteotomies. It was simulated a 42-C3 fracture, and that, after the restoration of length, alignment and rotation of the two major fracture ends, were fixed with a bridge plate with 12 holes having a working length corresponding to 4 holes.

Although the relative movements are more than 1 *mm* opposite to the plate, the specific movements by report to the distance between the main fragments are maintained between 2-3% which creates a true biological environment favorable to healing indirect (figure no. 12, 13). Note strain values below 2% immediately by the plate, a reason for the absence of periosteal callus in the vicinity of the plate - the other reason is related by disruption of local biological environment.

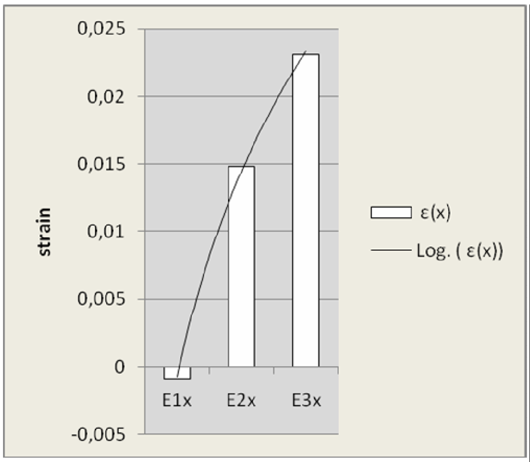

Figure 12: Longitudinal strain

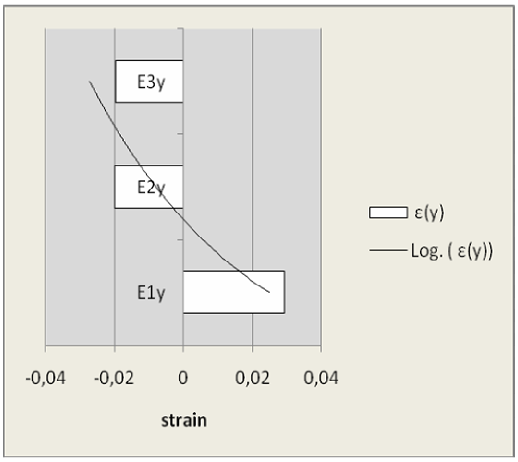

Figure 13: Radial strain

5. To evaluate the biomechanical comportment of a *external fixation device*, six levels were selected to perform measurements, ε (X, Y) for strain between the main fragments, i.e. ε $(X, Y)_i$ for strain between intermediate fragment against one of the main fragments..

External fixator takes over the longitudinal deformation and leads to a very strong, diverge, eccentric compression loading with great arm of forces (figure no 14, 15 – next page). Strain ranges between 0-3% create a different mechanical environment at different points of fracture. Deformation values in this experiment were of secondary importance, knowing the influence of external fixator stiffness characteristics on the biomechanical environment in the fracture gap. Chao 1982

6. To test the *reamed endomedullar nailing* it was performed a classical Kuntscher nail fixation of a fracture AO type 42-A2, simulated by a 45° oblique osteotomy. The reaming was undersized to avoid weakening incompatible with the needs of the experiment (it was use preserved bones). Measurements were performed in six pairs of points from which were extracted three series. The charts 16 and 17 are the results of strain after the system reached a steady state by telescopic - effect itself limited by fracture stability (Figure no 16 and 17 – next page).

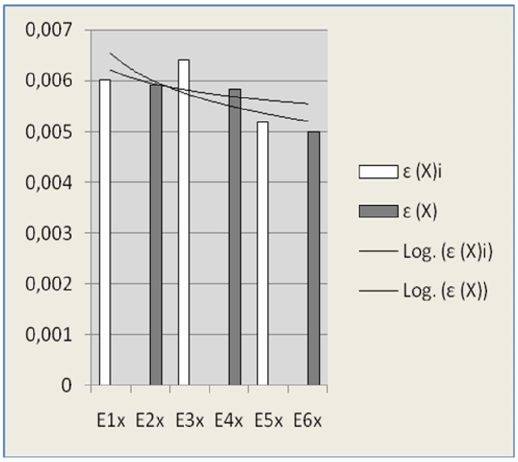

Figure 14: Strain in fixator plane (item 5)

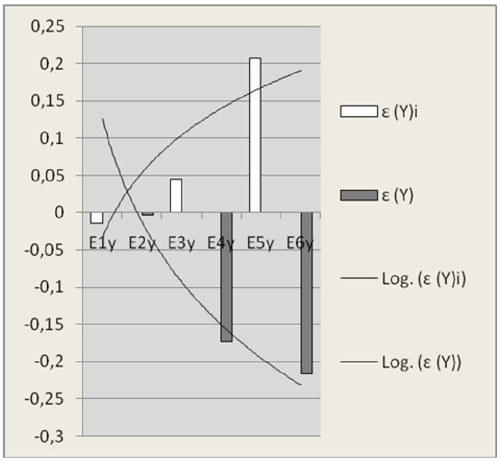

Figure 15: Strain on perpendicular plane (item 5)

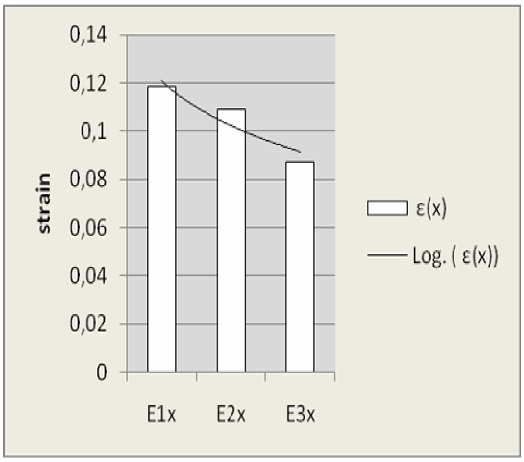

Figure 16: Longitudinal strain (item 6)

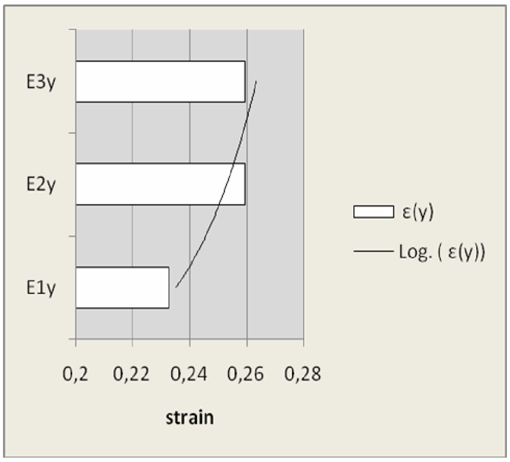

Figure 17: Radial strain (item 6)

From the two graphics the strains, ε_y and ε_x slide effect is found on the fracture slope. Equal effect occurs at an osteotomy angle of 45°; with increasing angle increases strain ε_x. The effect of endomedullar calibrating by reaming is the second important variable in obtaining of these values. Longitudinal strain decreases over time and after a few loading cycles stabilizes within the favorable micro-movements promoting indirect healing (see relative displacement evolution after the first 4 cycles of loading, in figure no. 18, a. and b.).

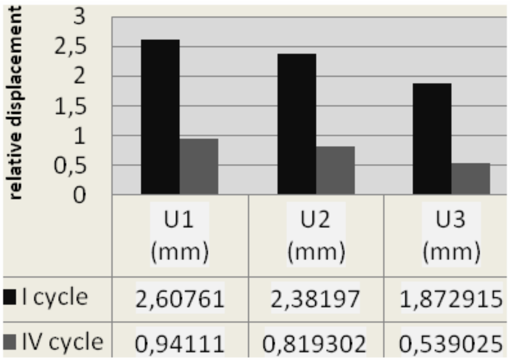

Figure 18a

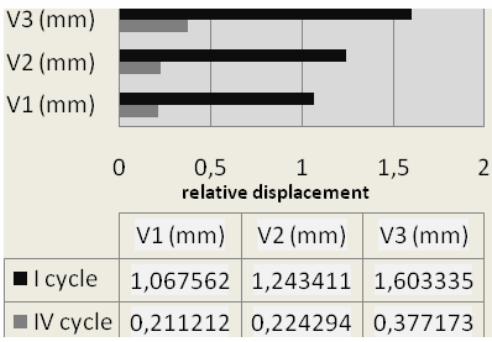

Figure 18b

Figure 3: Progressive stabilization of the system during the first 4 cycles of loading / unloading

Later, the osteotomy site has been transformed - by a further osteotomy - an AO type 42-B2. New instability conditions were created after the stabilization of first system. Main fragments have initially a rearrangement on the slope (obviously dependent on the angle osteotomy). In addition, intermediate fragment is moving and because of the effect by an inclined plane and wedge effect. For this reason, radial displacements (y) are two orders by magnitude higher, marking the axial and transverse instability complex in the fracture site. Instability is incompatible with osteonal healing (figure no. 19, 20).

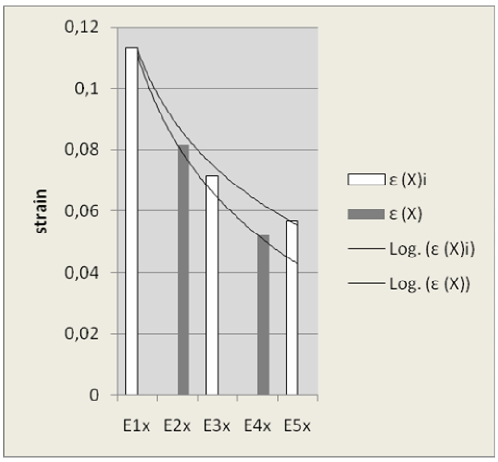

Figure 19: Longitudinal strain

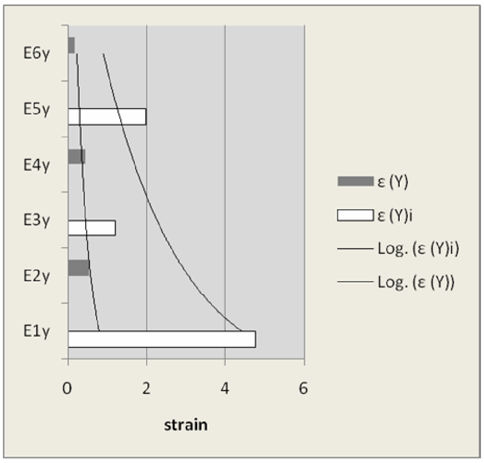

Figure 20: Radial strain

7. Secant arch fixation by *elastic nails* is by excellence a biologic one through minimally invasive approach and protects vascular networks but also by promoting favorable micro-movements by fracture fixation arc secant elastic nails suffer from mechanical point of view in terms of stability. Elastic nail fixation for unstable fracture was set in a difficult goal to achieve. Attempts to stabilize the elastic fixation had two directions: the combination of methods with internal fixation (cerclage, tension band) or external fixation, or fixation of nail ends with various methods by anchoring. In the following two sets of experiments we tested the behavior of this type of fixation where in the case of stable simple oblique osteotomy (42-A2) and secondary in the case of a wedge osteotomy (42-B2).

In a stable situation longitudinal strain (ε_x) create by the two elastic nails unequal intermittent compression effect (figure no. 21, 22). Radial it can observe a bending effect due to an eccentric position of the elastic nails in the medullar canal. After the fracture became unstable it can be observed shortening of complex, permanent translational and rotational displacements, with residual deformity incompatible with osteonal healing.

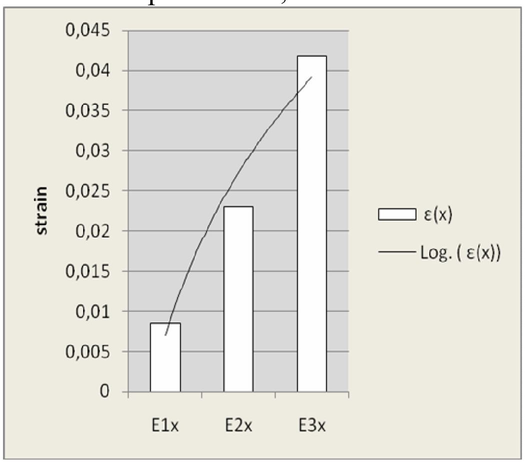

Figure 21: Longitudinal strain

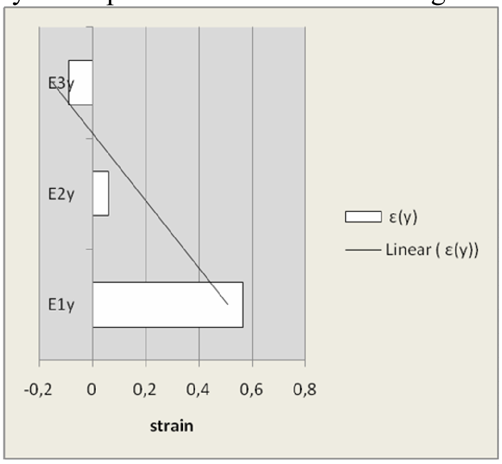

Figure 22: Radial strain

8. In the *undreamed locking nail fixation* the whole effort of displacement on oblique plane is controlled by specific shortening of the nail and over bloated effect of locking hole. The system is perfect balanced as longitudinal strain recorded similar ε_x in three points (figure no.23). The strain recorded in radial direction (figure no.24) is the effect of bending (eccentric compression applied).

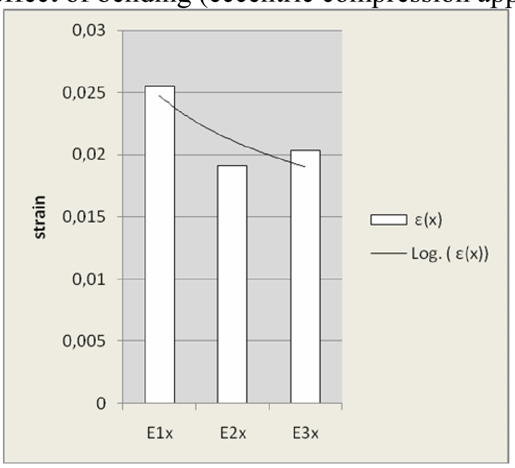

Figure 23: Longitudinal strain

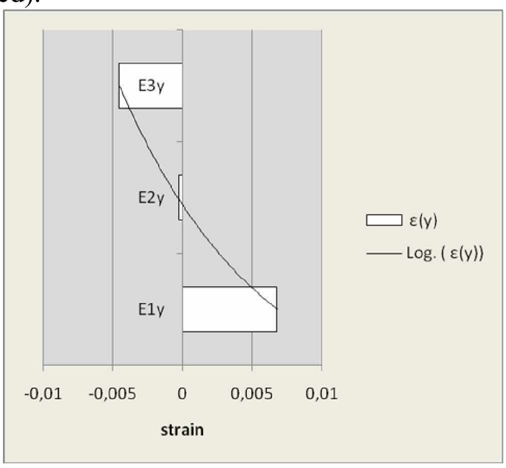

Figure 24: Radial strain

9. *LCP plate fixation as an internal fixator* was applied in a disproportionate assembly by bone diameter - double that of destination the plate - to achieve measurable and distinct values. To assess the biomechanical behavior of space in this report as a reference model - DCP plate was applied in the same configuration.

The strain in the longitudinal direction increases with distance by the plate while the radial direction have a pronounced bending phenomenon (ε_{3y} = 0,005). It can be seen in the last two cases analysis: the micro-movements appearance in the immediate vicinity of the titanium alloy plate (figure no.25, 26), while with chrome LCP plate in the neighborhood where virtually no micro-movements record (figure no.27, 28).

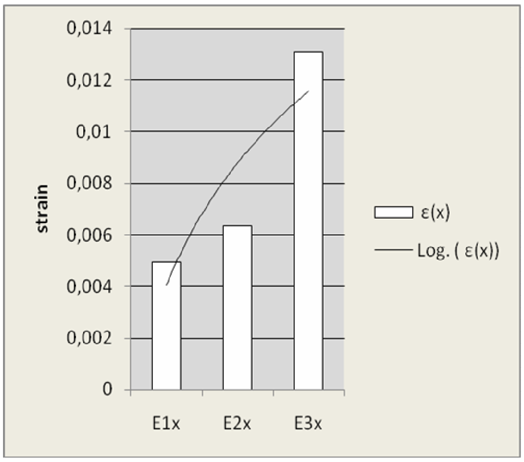

Figure 25: Longitudinal strain **(LCP_{Ti})**

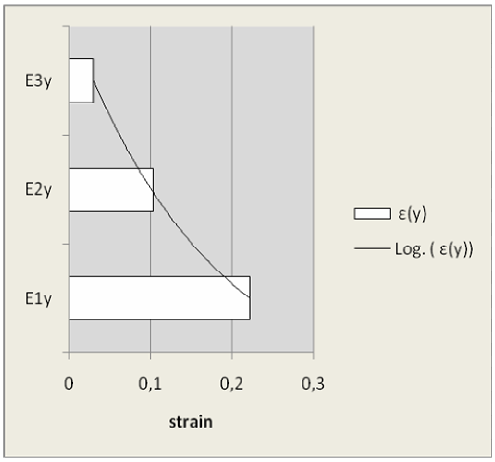

Figure 26: Radial strain **(LCP_{Ti})**

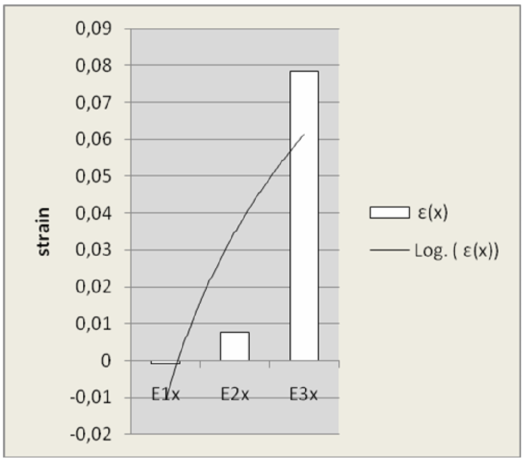

Figure 27: Longitudinal strain **(LCP_{Cr})**

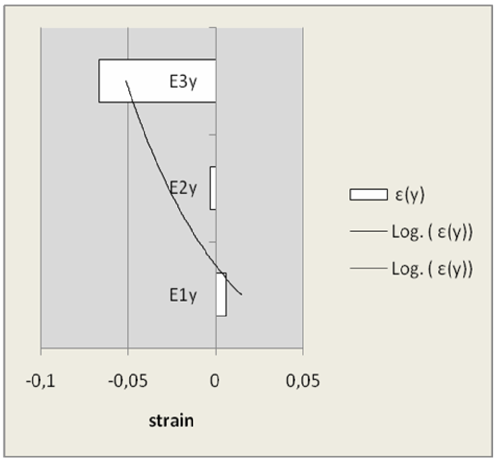

Figure 28: Radial strain **(LCP_{Cr})**

Discussion

The method of study is an experimental non-contact method, highly accurate with facility to use of their landmarks and do not require involvement of the linear displacement measuring instruments in any of the directions of investigation.

The field rigid fixation of shaft fractures with direct osteonal healing following the experimental evaluations is limited to the dynamic compression plate fixation with pre-bending (in type A1 fractures), and associating a lag screw in type A2 fractures; type B1 and B2 fractures can be fixed under rigid conditions with lag screw fixation combined with the protection plate.

Fixing on the principle of elastic bridge plate reach its biological role if the work segment provided a sufficient length (representing at least one third of the length of the plate) to promote micro-movements.

A particularly favorable environment for indirect healing is provided by the plate fixation on the principle of internal fixator. But, in conditions of increased stiffness plates (Cr), or in condition of inappropriate work length fatigue failure can occur. On the other hand close to the plate the gap shows the mechanical condition of absolute stability (one reason for the absence of callus in this area).

Flexible nail fixation (secant arch) promotes a biomechanical environment particularly favorable for osteonal indirect healing, with voluminous periosteal callus in condition of longitudinal variable intermittent compression along the fracture path, but only in axial stable fractures. Osteonal healing is incompatible with this type of fixation for unstable fracture; association with an additional means of stabilizing is mandatory.

Nail fixation through reaming calibration lead to indirect osteonal healing of simple fractures; even in the absence of perfect calibration stabilization occurs rapidly after the first loading cycles. In unstable fractures biomechanical environment is characterized by axial and rotational movement tending to the compatible limit for osteonal healing, but in vicious conditions (at least shortening and rotation).

Unreamed locked nail is a perfect way to stabilize the shaft fracture site but classical unreamed nail does not provide an ideal biological environment in terms of promoting micro-movements in fracture gap. This behavior explaine the late radiological callus appearance in unreamed static locked nail fixation. Improving the elastic quality of these nails in the active area can accelerate osteonal indirect healing by promotion favorable micro-movements.

Conclusion

Rigid fixation must meet one of three conditions: compression with lag screw, stabilization and compression by dynamic compression pre-bending plate, compression with lag screw associate protection plate.

Biomechanical, the ideal flexible fixation must to establish a stable and flexible milieu in fracture gap able to promote axial intermittent strain between 0.02 to 0.1 within early partial loading. A pertinent direction for the development of stable flexible fixation is to promote increase of elasticity in unreamed locked nailing.

References

1. Aalto, K., Holmstrom, T., Karaharju, E., et.al.: *Fracture repair during external fixation: Torsion test of rabbit osteotomies*. Acta Orthop. Scand. 1987, Feb, 58(1):66-70
2. Chao E.Y.S., Kasman R.H., An K.N., *Rigidity and stress analyses of external fracture fixation devices: A theoretical approach*. J Biomech 1982, 15:971-983
3. Gardner, M.J., Brophy, R.H., Campbell, D, et al. *The mechanical behaviour of locking compression plates compared with dynamic compression plates in a cadaver radius model*. J. Orth. Trauma, 2005, 19(9): 597-603
4. Hart, M.B., Wu, J.J., Chao, E.Y.S. and Kelly, P.J., *External skeletal fixation of canine tibial osteotomies: Compression compared with no compression*. J. Bone Joint Surg, 1985, 67A: 598 -605.
5. Hayes W.C., Girens W.B., Murch S.A. et.al. *Effects of plate modulus, thickness, and pre-bending on the mechanics of compression plate fixation*. Transactions of the 24th Annual Orthopaedic Research Society, Dallas, Texas, 1978
6. Hayes, W.C., Perren, S.M.: *Plate-bone fixation in the compression fixation of fractures*. Clin Orthop. Rel. Res., 1972, 89:236-240
7. Lewallen, D.G., Chao, E.Y.S., Kasman, R.A., et.al. *Comparison of the effect of compression plates and external fixators on early bone healing.* J. Bone Joint Surg.,1984, 66(7): 1084 -1091
8. Perren SM, Hayes WC - *Biomechanik der Platenosteosynthese*. Med. Orthop. Tech. 1974, 94:56-61
9. Perren SM. *Evolution of the internal fixation of long bone fractures. The scientific basis of biological internal fixation: choosing a new balance between stability and biology*. *J Bone Joint Surg Br*. 2002; 84(8):1093-1110
10. Perren SM. *Physical and biological aspects of fractures healing with special reference to internal fixation.* Clin Orthop Relat Res. 1979, (138):175-196
11. Rand, J.A., An, K.N., Chao, E.Y.S., et.al., *A comparison of the effect of intramedullary nailing and compression-plate fixation on fracture site blood flow and fracture union*. J. Bone Joint Surg., 1981, 63(3): 427-442
12. Slatis P, Karaharjn E, Holmstrom T et.al.: *Structural changes in intact tubular bone after application of rigid plates with and without compression*, J. Bone. Joint. Surg., 1978, 60(4):516-522
13. Wu, J.J., Shyr, H.S., Chao, E.Y.S., et. al.: *Comparison of osteotomy healing under external fixation devices with different stiffness characteristics*. J. Bone Joint Surg., 1984, 66(8): 1258-1264